frontiers | Frontiers in Marine Science

TYPE Original Research
PUBLISHED 04 April 2025
DOI 10.3389/fmars.2025.1558899

OPEN ACCESS

EDITED BY
Hong-Hai Zhang,
Ocean University of China, China

REVIEWED BY
Peng Zhang,
Guangdong Ocean University, China
Shan Jiang,
East China Normal University, China

*CORRESPONDENCE
Wentao Wang
wtwang@qdio.ac.cn
Yongbao Chu
941472609@qq.com

RECEIVED 11 January 2025
ACCEPTED 13 March 2025
PUBLISHED 04 April 2025

CITATION
Feng X, Wang W, Chu Y, Zhu J, Chi L, Chen J, Song X and Yu Z (2025) Study on the effect of modified clay on algae-derived organic nitrogen mineralization and its mechanisms in diatom *Skeletonema costatum*. *Front. Mar. Sci.* 12:1558899. doi: 10.3389/fmars.2025.1558899

Study on the effect of modified clay on algae-derived organic nitrogen mineralization and its mechanisms in diatom *Skeletonema costatum*

Xin Feng[1], Wentao Wang[2,3,4]*, Yongbao Chu[1]*, Jianan Zhu[2,3], Lianbao Chi[2,3], Jing Chen[2,3,4], Xiuxian Song[2,3,4] and Zhiming Yu[2,3,4]

[1]School of Environment and Safety Engineering, Qingdao University of Science and Technology, Qingdao, Shandong, China, [2]CAS Key Laboratory of Marine Ecology and Environmental Sciences, Institute of Oceanology, Chinese Academy of Sciences, Qingdao, China, [3]Laboratory for Marine Ecology and Environmental Science, Qingdao Marine Science and Technology Center, Qingdao, China, [4]College of Marine Sciences, University of Chinese Academy of Sciences, Beijing, China

Algae-derived organic nitrogen (AON) is mineralized by microorganisms to bioavailable inorganic nitrogen form, potentially sustaining the harmful algal blooms (HABs) for extended durations. The modified clay (MC) is an effective approach for mitigating HABs; however, its effects on the AON mineralization and the underlying mechanism remain unclear. In this study, the effects of MC on the mineralization of AON by a typical HAB species *Skeletonema costatum* were analyzed using the isotope dilution method, and the underlying mechanism were preliminarily discussed. The results revealed that the addition of MC could reduce the mineralization rates of AON and the regeneration amount of inorganic nitrogen by 71% and 60%, respectively, compared to the control group. The total fluorescence intensity was approximately 46% lower than that of the control group. In addition, the bacterial proliferation was suppressed by 66% and the community evolved from uniformity to diversification. It is hypothesized that the physical encapsulation of AON, chemical bonding of molecules and the variations of the microbial community under the utilization of MC were key mechanisms influencing the mineralization process. This study offers valuable insights into the environmental impacts following the HABs management and provides a scientific basis for investigating the controlling mechanisms of marine organic matter mineralization and burial.

KEYWORDS

modified clay, skeletonema costatum, algae-derived organic nitrogen, nitrogen mineralization, bacterial community

1 Introduction

Harmful algal blooms (HABs) are ecological anomalies caused by the proliferation or aggregation of planktonic microalgae living in seawater or freshwater. Studies have shown that the frequency of HABs and the area of a water body affected by HABs have increased dramatically, with the total affected area reaching as high as 31.47 million km^2 (Dai et al., 2023). At the end of HABs, a large amount of algal organic matter undergoes rapid microbial oxygen depletion and mineralization, causing anoxic acidification and secondary eutrophication in coastal waters (Feely et al., 2010; Cai et al., 2011; Wang et al., 2017), and this HAB phenomenon jeopardizes the local aquaculture industry, tourism, marine ecological safety and human health in a variety of ways (Testa et al., 2013).

Notably, the mineralization process is particularly intense at the end of HABs, where approximately 2–50% of algae-derived organic matter permeates into the surrounding water column via metabolic and cytolytic mechanisms (Thornton, 2014), and algae-derived organic nitrogen (AON) is generally not available for direct phytoplankton uptake and use (Lu and Ji, 1996; Berman and Bronk, 2003; Bronk et al., 2007). This organic matter is broken down by bacteria and released into the water column as bioavailable nitrogen (DIN_{bulk}, NH_4^++NO_2^-+NO_3^-, referred to as DIN_{bulk} hereafter). The liberated nutrients are capable of further fostering the growth of phytoplankton and microbial communities (Bertilsson and Jones, 2003), which in turn may lead to the sustained eutrophication of the water body (Pivokonsky et al., 2012; Zhou et al., 2019). For example, in the estuarine delta region of the Mississippi River, it has been estimated that approximately 40–60% of the organic matter in the estuary is mineralized and decomposed in the sediments, releasing nutrients such as inorganic nitrogen that support approximately 30–50% of the primary productivity of the region (He et al., 2023; Zhou et al., 2024). Through their participation in biological and microbial pumps, microorganisms mediate the marine organic matter cycle and play a significant part in the mineralization of nitrogenous organic matter (Jiao et al., 2011). In addition, AON with high bioactivity can rapidly stimulate microbial metabolic activity, resulting in hotspots of heterotrophic transformation, whereas AON with low bioactivity facilitates the long-lasting burial of sedimentary organic matter (Guo et al., 2023). This interaction between AON and bacterial communities influences the marine biogeochemical cycling (Chen et al., 2020).

Modified clay (MC) methods are currently the only methods that can be applied at large scales in the field in China in response to large-scale outbreaks of HABs (Yu et al., 2017). This method modifies the surface of clay particles, which the negative charge on the clay surface was converted to positive charge, and the bridging effects between clay particles and HABs were strengthened to achieve direct flocculation and sedimentation of HABs, thus effectively inhibiting the proliferation of algal cells. One key question that needs to be explored in practical application of MC methods is as follows: is the treated AON continuously converted into inorganic nutrients through mineralization, triggering secondary outbreaks of HABs after treatment? Recent laboratory studies have shown that the MC-based treatment of diatom blooms reduces the conversion of dissolved organic nitrogen to ammonia nitrogen, which in turn may mitigate the decomposition process of organic matter (Lu et al., 2017). In addition, it has been demonstrated by previous studies that small mineral particles occupy a crucial role in sequestering residues during organic matter mineralization (Jenkinson, 1977; Sorensen, 1981). To date, few studies have explored the process of mineralization of AON or the influence and mechanism of action of the mineralization process following the effects of MC. Moreover, there are still some general knowledge gaps, such as do the effects of MC influence the mineralization of organic nitrogen in microalgae and what are the mechanisms that affect the mineralization process? Addressing these questions will aid in assessing the marine nitrogen balance after the addition of MC, which is essential for maintaining ecosystem stability and environmental health.

To answer the above questions in depth, experiments related to the effects of MC addition on the mineralization process of a typical harmful algae, *Skeletonema costatum (S. costatum)*, were performed in a laboratory system, with a focus on the rate, content, and controlling mechanism, to provide data support for assessing the long-term effects of MC treatments on HABs. This study provides new findings regarding the factors that influence the mineralization and burial of marine organic matter.

2 Materials and methods

2.1 Microalgal culture and preparation of modified clay

MC (kaolin:PAC = 5:1) was prepared by modifying the surface of kaolin with the inorganic polymer polyaluminium chloride (PAC), as previously described (Yu et al., 1994). Kaolin clay was obtained from Bintang Puspita Bumidwipa Co., Ltd. (Bandung, Indonesia). PAC was purchased from Tianjin Guangfu Fine Chemical Company (Tianjin, China).

To eliminate the effects of other sources of dissolved organic matter (DOM) in seawater, the microalga *Skeletonema costatum* (*S. costatum*, obtained from the Chinese Academy of Science Key Laboratory of Marine Ecology and Environmental Sciences) was cultured in artificial seawater (ASW) at 20 ± 1°C, with 65 μmol photons m^{-2} s^{-1}, and over a 12:12 h light–dark cycle.

2.2 Experimental design

To simulate the real situation of algal death as best possible, the experiment was carried out when the algae were in the plateau phase. Since DIN_{bulk} (NH_4^++NO_2^-+NO_3^-) represents all bioavailable nitrogen, we treated the entire DIN_{bulk} pool production as total mineralization; therefore, the transformation process between inorganic nitrogen compounds was not considered in this study. Thus, we needed to measure only the entire DIN_{bulk} concentration and isotopic changes in the system. In addition, to

prevent the growth of algae and the photodegradation of organic matter from interfering with the experiment, we cultivated the algae in the dark during the experiment. The specific experimental procedure was as follows: 20 L of *S. costatum* was mixed in an acid-cleaned high-density drums, and then the isotope marker $^{15}NH_4Cl$ (≥98 atom%, Sigma–Aldrich, St. Louis, MO, USA) was added. The final concentration was approximately 10–15% of the DIN_{bulk} concentration in the system (Huang et al., 2022), which was calculated as 10%. The mixture was mixed and added to 75 square breathable cell culture bottles (75 cm^2, Nest) for 30 days for mineralization experiments. The long-term mineralization of the algal mixture without the addition of MC was considered to establish the control group. For the experimental group, the optimal MC concentration of 0.5 g/L was added, and three replicates of both groups were established. The samples were placed in a dark environment, and the temperature was set at 20~25°C for cultivation. All culture bottles were in contact with the atmosphere. The dynamics of the parameters in the system were analyzed by collecting water samples at different points in time during the 30-day mineralization process.

Samples were collected at 0 h, 3 h (1 day), 6 h, 9 h, 12 h, 24 h (2 days), 48 h (3 days), 5 days, 7 days, 10 days, 15 days, 20 days, 25 days, and 30 days. Unfiltered culture fluid was collected for the determination of TN, algal density, viable chlorophyll fluorescence, pH, and DO. Filtered culture fluid was collected for the determination of TDN, dissolved inorganic nutrients and AT $\%^{15}N/^{14}N$- DIN_{bulk}. The samples were collected at 0 and 6 h and 5, 7, 15, and 30 days, filtered culture fluid was used to analyze organic matter composition (using the fluorescence-dissolved organic matter [FDOM] fraction as a proxy), and unfiltered samples were used to analyze bacterial abundance (BA). The above filtrate samples were filtered through 0.7-μm-pore Whatman™ glass fiber filters (GF/F) (pretreated at 450°C for 5 h). In addition, 100 mL of algal sap was collected, and 0.2-μm polycarbonate membranes were used for bacterial community structure analysis. Three parallel samples were taken from each group, and the samples were shaken well during the sampling process. Prior to the incubation experiments, all the glassware was prerinsed with 10% v/v HCl for 24 h to remove possible contaminants, thoroughly rinsed with Milli-Q water, and precombusted at 450°C for 5 h.

2.3 Sample analysis

2.3.1 Determination of nutrients and environmental effects

The concentrations of dissolved inorganic nutrients (mainly nitrogen, phosphorus and silicon) were analyzed with a continuous flow analyzer (Skalar San++, The Netherlands). The TN and TDN samples were pre-digested with alkaline potassium persulfate prior to nutrient analysis. The data were evaluated via commercial nutrient reference materials to control the data quality. The cell density, pH, DO and *in vivo* chlorophyll fluorescence (Fa; Fluorescence Turner Designs, TD700, Sunnyvale, CA, USA) of the algal cultures were simultaneously monitored during the cultivation and flocculation periods. The cell densities were fixed with Lugol's reagent, and the cells were counted via a light microscope (OLYMPUS IX71, Japan).

2.3.2 Determination of AT$\%^{15}N/^{14}N$- DIN_{bulk}

The transformation process among inorganic nitrogen compounds, such as nitrification, were not considered in this study; only the overall DIN_{bulk} concentration and isotopic changes in the system were measured. The mineralization rates of AON (NMR) were measured by isotope dilution method. For calculating the mineralization rates of AON, the AT$\%^{15}N/^{14}N$-DIN_{bulk} were measured, which represented for the ratio of ^{15}N and ^{14}N atoms in the DIN_{bulk}. This parameter was determined via the sodium hypobromite–denitrifying bacteria coupling method (Sigman et al., 2001). Specifically, the samples were pre-treated with sodium hypobromite solution to fully oxidize NH_4^+ to NO_2^-, and then, denitrifying bacteria were used to convert both NO_2^- and NO_3^- in the system to N_2O, which was finally analyzed via isotope ratio mass spectrometry (Delta V Advantage; Thermo Fisher Scientific Inc., USA) to determine the nitrogen isotopic composition of N_2O. The precision of measurements were tested by using the USGS 34, USGS 32, and IAEA-N3 isotope standards.

2.3.3 Determination of FDOM composition

The main components of FDOM were analyzed via fluorescence spectroscopy coupled with parallel factor (PARAFAC) analysis (Li et al., 2018). The excitation emission matrix (EEM) of the samples was determined via a fluorescence spectrophotometer (Hitachi F-4600) with an excitation wavelength (E_x) of 200–600 nm at 5 nm intervals and an emission wavelength (E_m) of 200–700 nm at 5 nm intervals. The scanning speed was 12000 nm/min (Stedmon et al., 2003). MATLAB (MathWorks, Natick, MA) together with the DOM Fluor toolbox (http://www.models.life.ku.dk/) were employed for data analysis (Coble, 1996; Coble et al., 1998).

2.3.4 Bacterial abundance and bacterial community structure analysis

BA samples were fixed with glutaraldehyde at a final concentration of 0.5% and stored at -80°C. BA was determined via SYBR Green I staining (1:10,000, V/V) with a fluorescence microscope (OLYMPUS DP73, Japan) in the dark. Bacterial enumeration was performed as previously described (Noble and Fuhrman, 1998).

Microbial DNA was extracted via HiPure soil DNA kits (Magen, Guangzhou, China) according to the manufacturer's protocol. After DNA extraction, PCR amplification (16S rDNA V3-4 region), purification, and quality testing, all the qualified samples were used to construct sequencing libraries. Specifically, the 16S rDNA target region of the ribosomal RNA gene was amplified via PCR with the V3–V4 universal primers 341F (5′-CC TACGGGNGGCWGCAG-3′) and 806R (5′-GGACTACHVGGG TATCTAAT-3′), and sequencing was performed on the Illumina platform (PE250). Data were analyzed to identify and quantify bacterial species at the compendium level. Clustering of operational

taxonomic units (OTUs) was performed with 97% concordance (Identity), and then the sequences of the OTUs were annotated for each species. The annotation database used was Silva 138.1. Alpha diversity was assessed via the Shannon index. Two-way analysis of variance (two-way ANOVA), together with Tukey's *post hoc* test, and permutational multivariate analysis of variance (with the Adonis function) were performed to examine differences in alpha diversity and community composition among the experimental treatments and over time. Annotation and prediction of bacterial community functions were performed on the basis of OTU taxonomic lists obtained from the FAPROTAX database (Laura and Louca, 2016).

2.4 Statistical analysis

The formulas for calculating various nitrogen concentrations are given in Equations 1–4 below:

$$DIN_{bulk} = NH_4^+ + NO_3^- + NO_2^- \quad (1)$$

$$DON = TDN - DIN_{bulk} \quad (2)$$

$$PON = TN - TDN \quad (3)$$

$$TON = DON + PON \quad (4)$$

Here, NH_4^+, NO_3^-, and NO_2^- represent the concentrations of ammonium, nitrate, and nitrite (μM), respectively, and TN and TDN represent the concentrations of total nitrogen and total dissolved nitrogen (μM), respectively. The above data were measured with test equipment (Skalar San++, The Netherlands). DIN_{bulk}, DON, PON, and TON represent the concentrations of dissolved inorganic nitrogen, dissolved organic nitrogen, particulate organic nitrogen, and total organic nitrogen (μM), respectively.

The mineralization rate of AON (NMR) in this study was determined according to the modified rate equation of Kirkham and Bartholomew (1954); in this isotope dilution method, it is assumed that the decrease in ^{15}N enrichment in the DIN_{bulk} pool is due to the dilutional effect of nitrogen mineralization:

$$NMR = \frac{Mi - Mf}{\Delta t} \times \frac{log\,(Ni/Nf)}{log\,(Mi/Mf)} \quad (5)$$

where NMR (μM/h) refers to the instantaneous mineralization rate of AON; M_i and M_f (μM) are the total DIN_{bulk} concentrations at moments i and f; and N_i and N_f refer to $AT\%^{15}N/^{14}N$- DIN_{bulk} in the samples at moments i and f. Δt (h) refers to the difference in incubation time (f-i). All M values can be calculated via Equation 1. All N values were obtained from isotope mass spectrometry data.

PARAFAC for all samples of the dissolved organic matter fraction in this study was performed via MATLAB (version R2023b; Mathworks, USA) and the drEEM toolbox. Prior to analysis, spectral correction, correction for internal filtration effects and deduction of ultrapure water blanks were performed on the matrices via the 'fdomcorrect' function in the drEEM toolbox. The fluorescence intensity of the EEM matrix was normalized (R.U.) at an excitation wavelength of 350 nm via the Raman spectral peak area of water. The Raman and Rayleigh scattering regions were eliminated and replaced according to the interpolation method used by Murphy et al. (2013). In our study, the reliability of the four-component model was verified by split-validation analysis and random initialization analysis, as well as analysis of residuals (Stedmon and Bro, 2008) (Supplementary Figure S1).

Data processing and graphing were performed via Origin 2024b (version 2024b; OriginLab, USA).

3 Results

3.1 Characteristics of changes in TON and DIN_{bulk}

The mineralization process was accompanied by organic and inorganic changes, and the changes in the two groups were observed. The total organic nitrogen (TON) concentrations in both the control and experimental groups displayed a decrease tendency the incubation time lengthened (Figure 1A), and the TON concentrations of the control and experimental groups ranged from 149.51 to 218.81 μM and from 180.38 to 218.81 μM, respectively. The findings demonstrated that the DIN_{bulk} concentration within the control group under dark incubation conditions tended to fluctuate with increasing incubation time (Figure 1B) and initially increased from 233.54 to 261.28 μM on the 30th day. In general, DIN_{bulk} in the control group increased fastest in the first 7 days. The DIN_{bulk} concentration in the experimental group generally slowly increased. As the incubation time increased, the DIN_{bulk} concentration changed more moderately, and the concentration on day 30 was 244.53 μM. At the later stages of incubation, the concentration of DIN_{bulk} in the experimental group was less than that in the control group. Overall, the experimental group presented high TON concentrations and low DIN_{bulk} concentrations compared with those of the control group.

3.2 Characteristics of changes in nitrogen mineralization rates

To accurately determine the rate of AON mineralization, we applied an isotope dilution method to correct the rate of mineralization. The percentages of ^{15}N and ^{14}N in the two groups during incubation tended to decrease over time (Figure 2A). In this case, the values for the two groups decreased rapidly from the initial value 9.66 to 2.14 and 7.41, respectively, within 7 d, followed by slow decreases to 3.78 and 6.85 on day 30. The mineralization rate of AON (NMR) was calculated by substituting $AT\%^{15}N/^{14}N$ into Equation 5, and the variation with time is illustrated in Figure 2B. The NMR of the control and experimental groups fluctuated from 0.13–24.33 and 0.01–6.97 μM/h, with the highest values of NMR reaching 24.33 and 6.97 μM/h at 6h and 9 h, respectively, and then

10.3389/fmars.2025.1558899

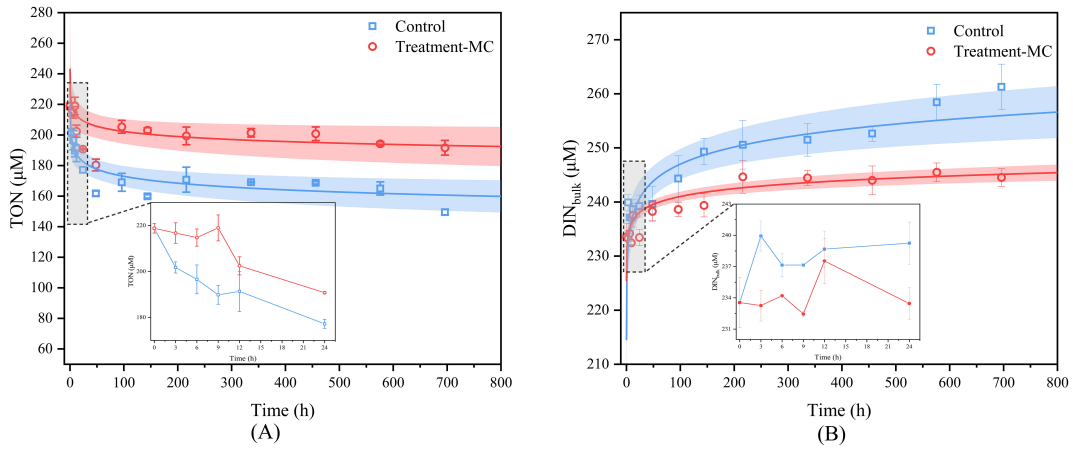

FIGURE 1
Dynamic changes of TON **(A)** and DIN$_{bulk}$ **(B)** concentration during MC conditioning.

gradually decreased. The mean values in one month were 7.04 and 2.07 μM/h, respectively. Upon adding MC, the mineralization rate decreased by 71% in comparison to that of the control group.

3.3 Characteristics of changes in environmental factors

Both the system DO and pH tended to decrease initially but then increased (Figures 3A, B). The initial DO of the system was 9.61, and the DO of the control and experimental groups decreased to minimum values of 7.09 and 7.13 at 7 d, respectively, and then slowly rebounded to 7.64 and 7.79, respectively. The initial pH of the system was 9.03, and that of the control group decreased to a minimum value of 7.97 at 10 d and then slowly rebounded to 8.05 at 30 d. After the addition of MC, the pH of the system rapidly decreased to 7.73, then decreased to a minimum value of 7.68 at 7 d, and then slowly rebounded to 7.85 at 30 d. There was little change in DO and a decrease in pH after the addition of MC compared with that in the control group.

The concentrations of inorganic phosphate (DIP) and inorganic silicate (DISi) gradually increased over time, from 1.04 and 21.68 μM to 2.30 and 46.74 μM, respectively, on day 30 within the control group the control group. The addition of MC resulted in a slow increase in the concentrations of DIP and DISi to 2.00 and 13.77 μM, respectively, on day 30 (Figures 3C, D). In contrast to the concentrations in the control group, the levels of inorganic phosphate and silicate decreased after the addition of MC.

3.4 Characteristics of changes in the organic matter fraction

Changes in the active fraction of organic matter affect its conversion to inorganic nitrogen, and PARAFAC analysis revealed four fluorescent components (Supplementary Figure S1).

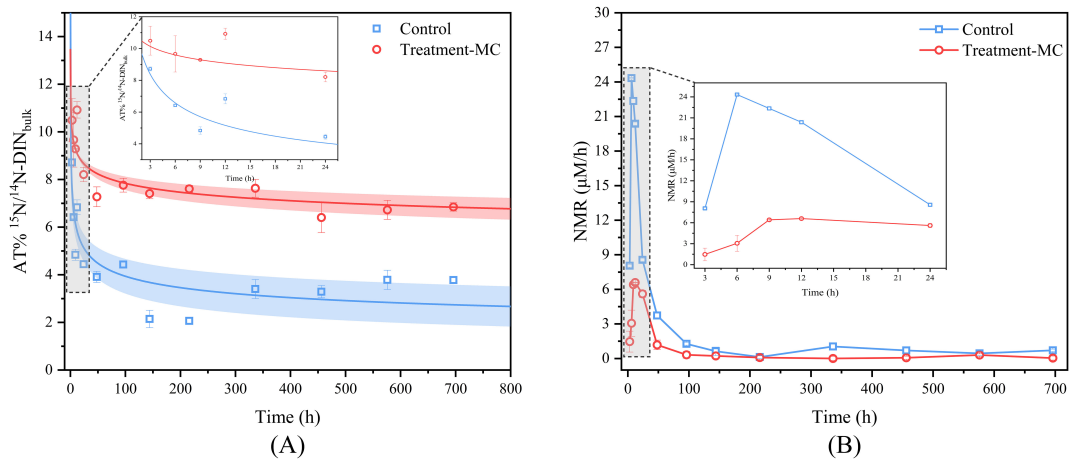

FIGURE 2
Dynamic changes of isotope and mineralization rate during MC conditioning (**A**. AT%^{15}N/^{14}N- DIN$_{bulk}$ changes; **(B)** mineralization rate changes).

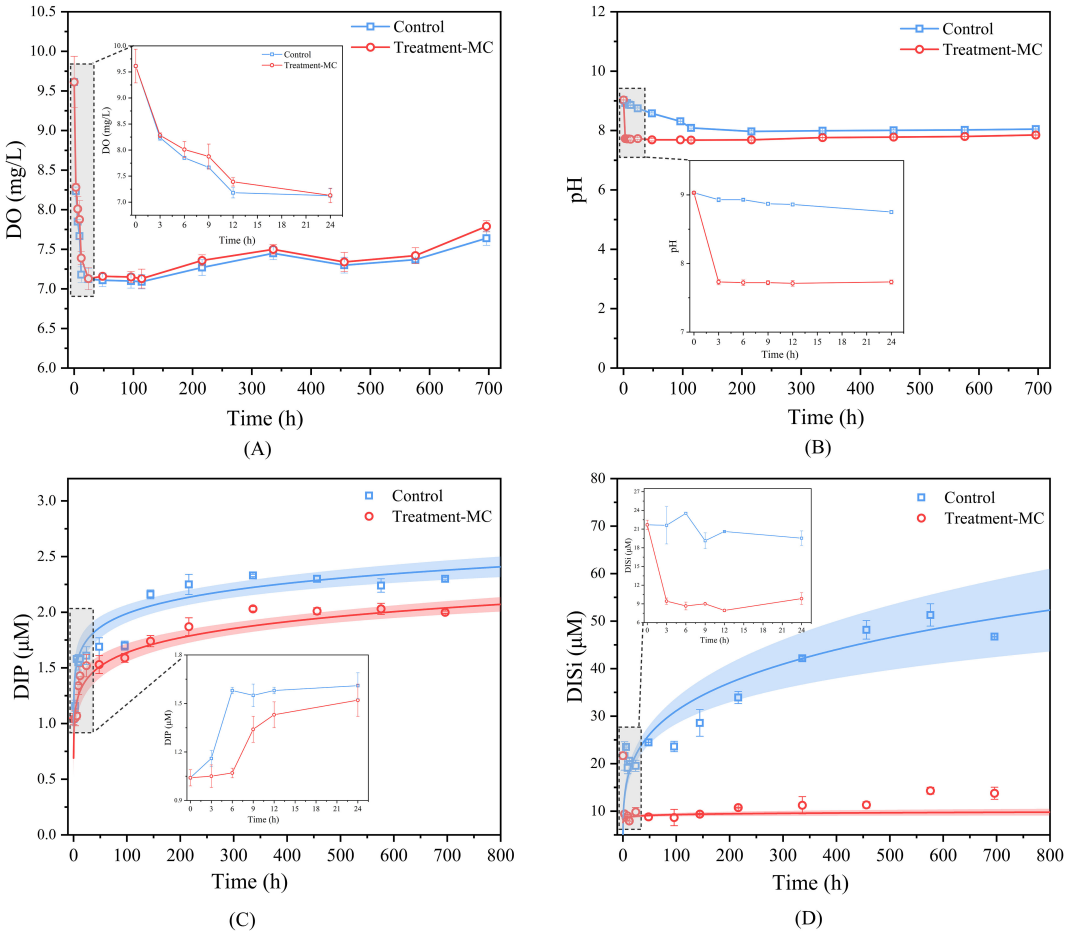

FIGURE 3
Dynamic changes of environmental factors during MC conditioning (**A**. DO change; **B** pH change; **C** inorganic phosphorus change; **D** inorganic silicate change).

The excitation/emission wavelengths of C1-C4 were 290 | 320 nm, 330 | 350 nm, 375 | 395 nm and 245 | 520 (285) nm, respectively (Supplementary Table S1). Among them, component C4 has one excitation peak, one strong emission peak and one weak emission peak (520 nm/285 nm), and the fluorescent components at the strong emission peak were mainly used to analyze component C4 in this study. According to the published models in the OpenFluor database (Murphy et al., 2013) and their wavelengths, C1 and C2 represent protein-like substances, and C3 and C4 represent different humic-like substances. Protein-like substances are often considered indicators of biologically liable nitrogenous organic matter, and humic-like substances are often considered potential tracers of recalcitrant nitrogenous organic matter (Romera-Castillo et al., 2011; Catalá et al., 2015). Therefore, we classified the four components into two groups: labile organic matter, represented by protein-like substances, and recalcitrant organic matter, represented by humic-like substances. Throughout the mineralization process, the dynamics of the fluorescence intensity of the two groups of protein-like substances manifested two phases (Figure 4A): the fluorescence intensity reached its peak value within 7 days and thereafter started to decrease until the end of the experimental cycle. Notably, the alterations in the humic-like substances exhibited an opposite tendency, where the values of both groups of humic-like substances progressively augmented throughout the mineralization process (Figure 4B).

We further analyzed the characteristics of the total FDOM in the two groups over time. The results revealed that the total FDOM in the control group increased rapidly to the peak value within 7 d and subsequently declined gradually until the final day (Figure 4C). The total FDOM in the experimental group fluctuated with time. On the basis of the total FDOM at the end of the experiment between the two groups, the total fluorescence intensity of the experimental group was approximately 46% lower than that of the control group.

3.5 Characteristics of changes in microbial abundance and community composition

The coupled process of organic matter mineralization and nutrient regeneration is mediated mainly by bacteria. The bacterial density in the control group increased continuously

10.3389/fmars.2025.1558899

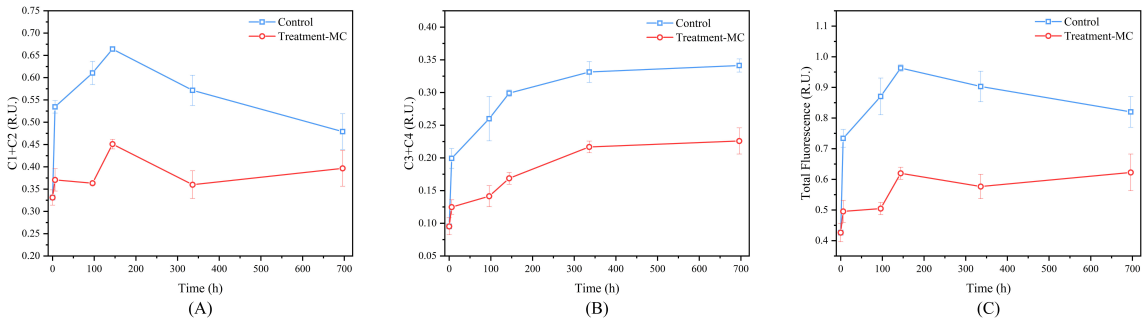

FIGURE 4
Dynamic changes in the main components of fluorescent dissolved organic matter (FDOM) during MC conditioning (**A**. changes in protein-like substances; **B** changes in humus-like substances; **C** changes in total fluorescence intensity).

from 3.30×10^9 cells/L at the beginning to 6.70×10^9 cells/L at the 7th d and then increased slowly to 7.40×10^9 cells/L at the 30th d. The bacterial density in the mixture decreased to 2.87×10^9 cells/L after the addition of MC and then fluctuated to 4.70×10^9 cells/L at the 30th d. Overall, the increase in microbial abundance was reduced by 66%. The Shannon index is often employed to evaluate the diversity of communities. The Shannon index of the experimental group was greater than that of the control group, i.e., the community diversity increased. Overall, the bacterial abundance in the experimental group was consistently lower than that in the control group, and the species diversity was more pronounced than that in the control group (Figures 5A, B).

In this study, the diversity of bacterial communities and their differences during culture were analyzed via the 16S rDNA technique. Heterogeneity in community composition and structure existed among the five time points of the two groups of microbial communities. Upon clustering the sequences into OTUs at the 97% similarity level, a total of 1317 OTUs were identified in the complete dataset. The bacterial community composition of each group at the class level is shown in Figures 5C, D. Without the addition of MC, the dominant bacteria in the algal mixture were *Alphaproteobacteria*. Over time, *Gammaproteobacteria* gradually appeared. However, after the addition of MC, the dominance of *Alphaproteobacteria* in the system diminished, and the proportion of *Gammaproteobacteria* augmented. The bacterial abundance gradually increased with time. The bacteria *Bacteroidia*, *Actinobacteria*, *Verrucomicrobiae* and *Planctomycetota* also appeared, and the abundances of all four bacteria increased gradually with time. On the basis of the functional annotations and abundance information of the samples in the database, the 16S

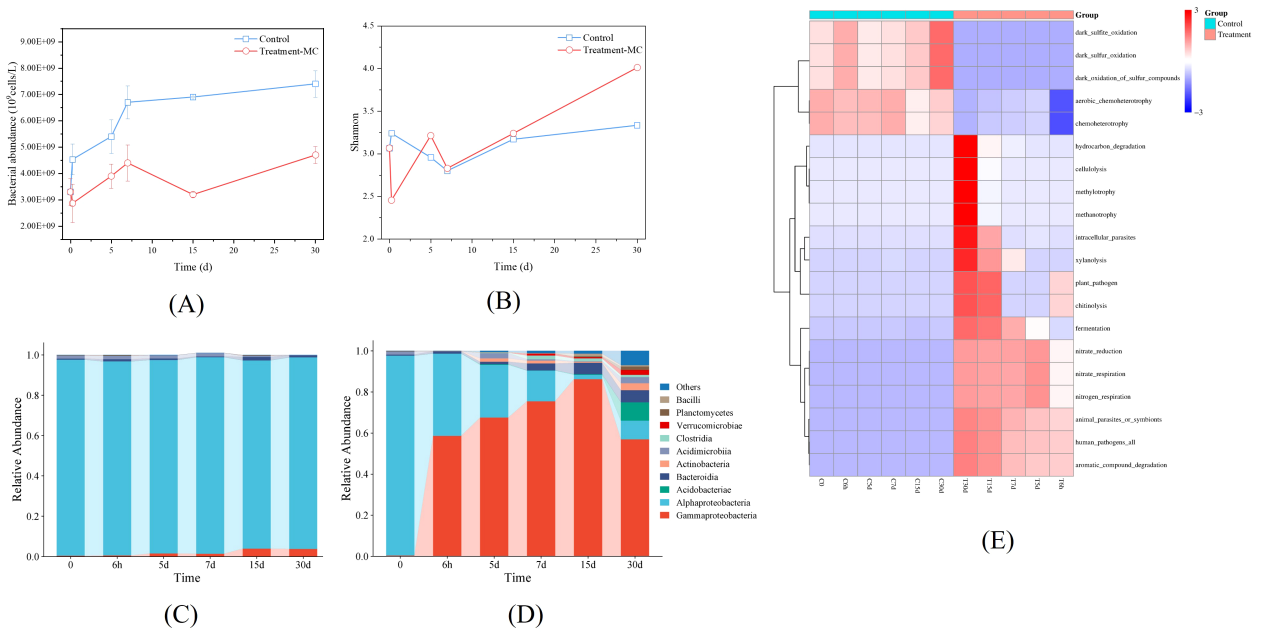

FIGURE 5
Dynamic changes of microbial during MC conditioning (**A**. change in abundance; **B** community diversity; **C** change in community composition at class level for the control group; **D** change in community composition at the class level for the experimental group; **E** functional prediction of the two groups of OTUs on the basis of FAPROTAX).

rDNA sequencing results were used to predict the functions of the bacteria via the FAPROTAX tool, and the top 20 functions in terms of abundance and associated information for each sample were selected to create a heatmap, with clustering at the level of functional differences, as shown in Figure 5E. Control group bacterial functions were related to chemoenergetic heterotrophy and sulphur oxidation (such as chemoheterotrophy, aerobic chemoheterotrophy and sulfite_oxidation). The experimentally observed bacterial functions were related to hydrocarbon, xylan and cellulose degradation.

4 Discussion

4.1 Mitigating effect of MC on the mineralization process of AON

Nutrient salts are an important basis for the occurrence of harmful algal blooms (Davidson et al., 2014), and mineralization process plays a crucial role in nutrient cycling. It is generally believed that particulate organic matter (POM) undergoes a two-step decomposition process under the action of microorganisms: most POM is first hydrolyzed by extracellular enzymes and converted into DOM, which can be utilized by microorganisms (BDOM), and then, labile DOM (LDOM) completely decomposes into dissolved inorganic salts, while the remaining recalcitrant DOM (RDOM) gradually accumulates (Jiao et al., 2010).

In this study, *S. costatum* was the main provider of AON, and the gradual death and lysis of algal cells under dark conditions resulted in a decrease in PON and increases in DON and DIN_{bulk} (Figures 6A–D), suggesting that the decomposition and conversion of particulate nitrogen to dissolved nitrogen occurred. After the addition of MC, the percentage of PON consistently increased, and the percentages of DON and DIN_{bulk} were consistently lower than those for the control group (Figures 6B), indicating that the conversion of particulate nitrogen to dissolved nitrogen was inhibited. As mentioned above, particulate organic matter undergoes a two-step decomposition process, and as the MC inhibits the conversion of particulate nitrogen to dissolved nitrogen, the amount of dissolved inorganic salt regenerated is

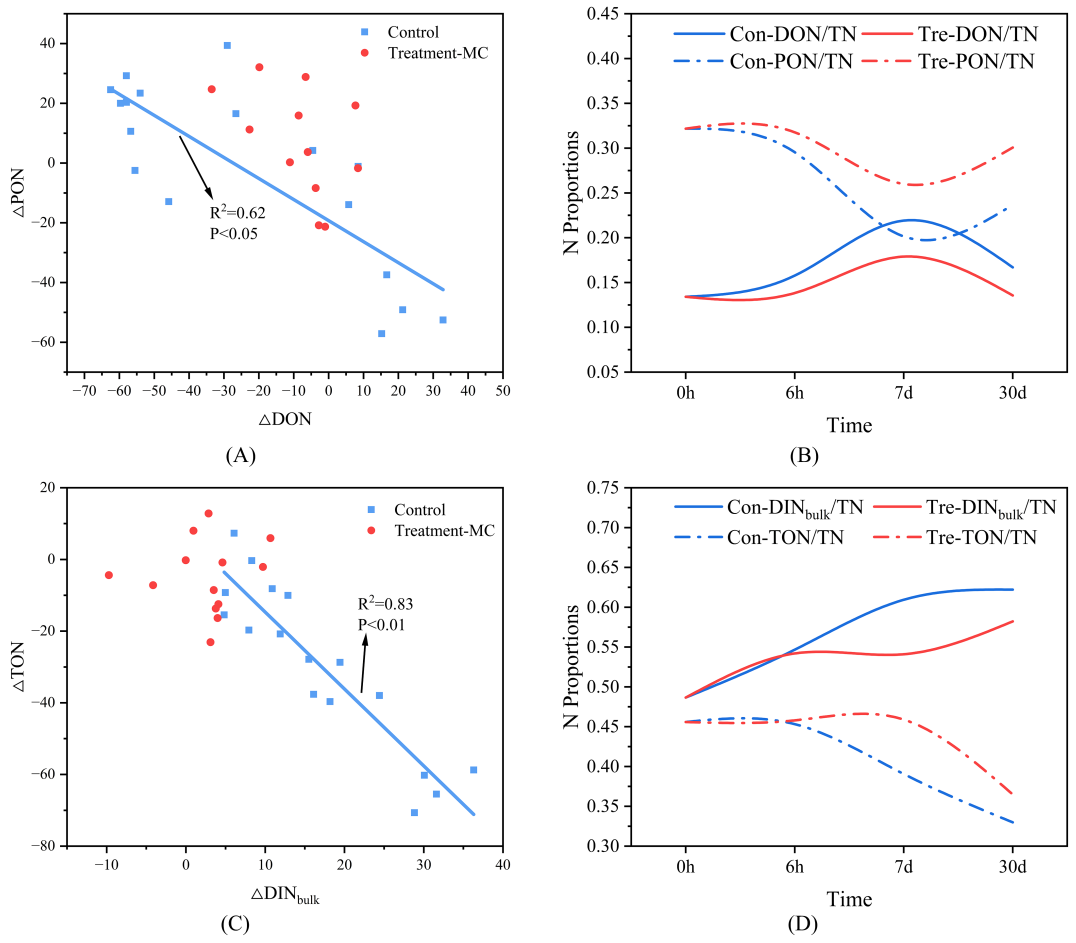

FIGURE 6
The effects of MC on the transformation between multiple nitrogen compounds (**A, C**: the relationship between the reduction in organic elements and the production of inorganic elements; **B, D**: the transformation of nitrogen forms; Con represents the control group; Tre represents the MC treatment group).

also reduced. We attempted to compare nitrogen content conversion, organic matter fractions and microbial abundance changes over the experimental cycle by dividing the experimental cycle into a pre (0-6h), mid (6h-7d) and post (7d-30d) period. The effect of MC showed variability in the inhibition of TON decomposition, DIN_{bulk} regeneration, mineralization rate, and microbial and AON growth at different time intervals (Figures 7A–E). Specifically, the most significant mitigating effects on TON decomposition, DIN_{bulk} regeneration, and mineralization rate were 82%, 82%, and 86%, respectively, within 6 h after MC addition. The mitigation of TON decomposition, DIN_{bulk} regeneration and mineralization rates diminished during the 7-day period, but the mitigation of microbial and AON growth increased. In the later stages, the inhibition of DIN_{bulk} regeneration and mineralization rates remained high, while the inhibition of microbial and AON growth stabilized between 34% and 44%. We hypothesis that MC achieved a slowing of the full-cycle mineralization process by inhibiting the decomposition of LDOM in the early stages and inhibiting microbial reproduction in the middle stages. Taken together, on a monthly scale, the addition of MC reduced both TON and DIN_{bulk} by 61% and 60%, respectively, and the mineralization rate decreased by 71% (Figure 7A). In addition, inorganic phosphorus and inorganic silicate were reduced by 76% and 32%, respectively (Figure 3). The decomposition in organic nitrogen and the regeneration of each dissolved inorganic salt were significantly reduced within 30 days of the addition of MC, and the mineralization of organic matter slowed. It is speculated that clay particles have a certain sequestration and protection effect on organic matter, which can delay the decomposition process of organic matter by microorganisms (Pinck and Allison, 1951; Eusterhues et al., 2003; Chi et al., 2022). The specific mechanism of this impact will be analyzed and discussed later.

4.2 Mechanistic analysis

4.2.1 The effects of MC on mineralization from an organic nitrogen perspective

The mineralization process involves the microbially regulated conversion of organic nitrogen from organic to inorganic forms. From the point of view of microbial availability, DOM can be roughly classified into DOM that is easily utilized and consumed by microorganisms within a few days or even hours (LDOM), semi-labile DOM (SLDOM), which is decomposed by microorganisms in months to years, and recalcitrant DOM (RDOM), which is difficult for microorganisms to utilize. RDOM can be stored for thousands of years (Jiao et al., 2010). As mentioned above, after microorganisms first hydrolyze the material, transitioning from a granular state to a dissolved state, the labile dissolved material is preferentially converted into inorganic salts. Thus, MC may mitigate the overall mineralization rate by limiting the bioavailability of organic nitrogen. The mode of mitigation may encompass both physical and chemical sub-modes of action.

In terms of the physical mode of action, since the AON carries a negative charge and the MC material carries a positive charge, the

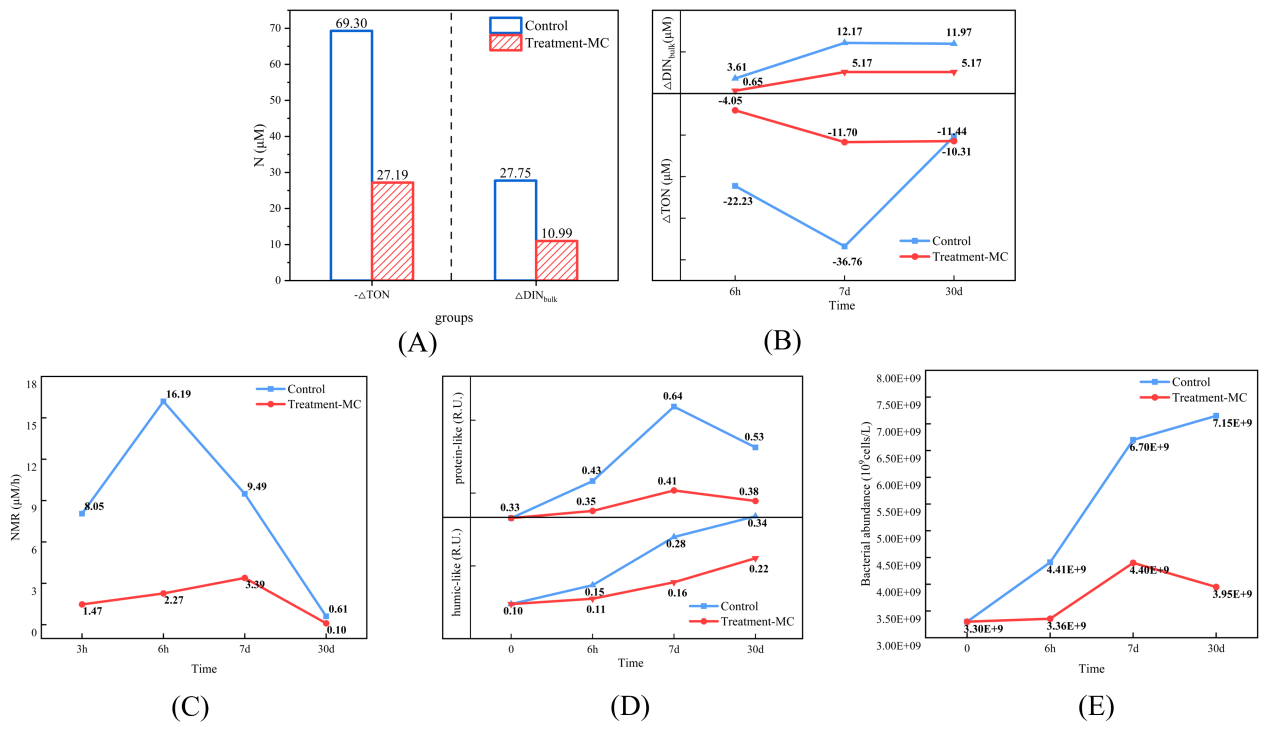

FIGURE 7
Comparison of effects of MC in pre (0-6h), mid (6h-7d) and post (7d-30d) period (**A, B** the total and process impacts of TON decomposition and DIN_{bulk} regeneration, respectively; **C** effects on NMR; **D** effects on organic matter fractions; **E** effects on bacterial abundance).

dissolved state of organic nitrogen can be combined with the clay by charge adsorption (Goring and Bartholomew, 1952; Pinck, 1962; Gibbs, 1983) and gradually form large particle size flocs together with the particulate matter during settling via adsorption bridging and sweeping netting (Lu et al., 2015; Chi et al., 2024). This formation of large flocs allows organic nitrogen to be encapsulated by MC (Lu et al., 2015; Chi et al., 2024) and to exist as a clay–organic matter complex. The physical protection of nitrogenous organic matter by this clay–organic matter complex (Hemingway et al., 2019) greatly limits the direct contact of organic nitrogen with microorganisms and reduces the number of contact surfaces and oxidative contact sites between organic nitrogen and microorganisms (Liao, 2006; Salter et al., 2011). In this study, the conversion of particulate to dissolved and organic to inorganic states slowed within 1 month (Figure 6). Liu et al. (2021) also demonstrated, through SEM images of cyanobacteria–clay copolymers, that cyanobacteria in the cyanobacteria–clay group remained well preserved over a month compared with those in the clay–free group. Therefore, it is speculated that the clay particles mitigated the mineralization of nitrogenous organic matter on a monthly scale.

In terms of the chemical mode of action, organic nitrogen may be chemically bonded to modified clays, leading to a relatively stable chemical structure for the clay–organic matter complex (Sorensen, 1981), which increases the difficulty of microbial decomposition and prolongs the microbial decomposition time for the mineralization of organic nitrogen. Organic molecules bind to the amorphous aluminium formed by the hydrolysis of MC, and *S. costatum* can incorporate aluminium into their siliceous shells (Koning et al., 2007), which reduces the rate of decomposition of the siliceous shells (Dixit et al., 2001; Beck et al., 2002; Cappellen et al., 2002), whereas aluminium continues to bind to *S. costatum* biomolecules to form strong bonding structures (Exley and Mold, 2015; Zhou et al., 2021a); this leads to difficulties in the dissociation and decomposition of *S. costatum*, thus prolonging the microbial decomposition of diatom organic matter. In addition, the adsorption of amino acids and sugars by surface ions on clay minerals increases the concentration of the two substances on the mineral surface, which are regarded as catalysts for condensation polymerization between amino acids and sugars (Gonzalez and Laird, 2004), facilitating humic substance formation (Zhao et al., 2023). The presence of humus-like organic matter, which is difficult for microorganisms to utilize, prolongs the microbial mineralization process and slows the mineralization rate (Figure 2B). This chemical bonding limits the bioavailability of AON, increases the difficulty of microbial mineralization, and can effectively mitigate the mineralization of AON.

4.2.2 Microbiological perspective on the effects of MC on mineralization

Microorganisms play an important role in the mineralization of organic matter by participating in the biological and microbial pumps that mediate the marine organic matter cycle. The high dominance of *Alphaproteobacteria* bacteria, which have also been reported to respond to diatom-derived DOM (Landa et al., 2014), was sustained in the control group during the 30 days of this study. Moreover, the presence of highly bioavailable AON in large quantities provides a rich source of nutrients for mineralizing bacteria, and while nutrients are degraded by bacteria, a portion of them are converted into bacterial biomass, contributing to an increase in bacterial abundance (Chen et al., 2020; Zhou et al., 2021b). However, rapid resource depletion may favor some specific bacterial taxa (Pekkonen and Laakso, 2012), and it is observed that the bacterial diversity in the control group increased slowly due to the widespread presence of *Alphaproteobacteria* (Figure 5). In addition to being converted into bacterial biomass, a substantial portion of the released nitrogenous organic matter is released as CO_2 via microbial respiration, leading to a decrease in system pH (Chen et al., 2020). Moreover, as the mineralization of bacteria consumes oxygen and decreases the system DO (Figure 3A), *Gammaproteobacteria* begin to proliferate (Dyksma et al., 2016). Both types of bacteria have chemoheterotrophic bacterial functions. This group of bacteria is responsible for 75% to 95% of the decomposition of organic matter in the ocean (Kothawala et al., 2021; Yang et al., 2024) and is capable of decomposing a wide range of nitrogen-containing organic compounds, such as sugars, amino acids, and humic substances (Fuchs et al., 2011). The increase in inorganic salts in the control system occurs in conjunction with the increase in the abundance of chemoheterotrophic bacteria.

The addition of MC influenced the microenvironment of the water body, which led to a decrease in the abundance of *Alphaproteobacteria* bacteria at the dominant site, possibly because MC can filter some free microorganisms (Ding et al., 2021). The small decrease in the pH of the water body may allow *Gammaproteobacteria*, which are well adapted to the water environment, to gradually proliferate (Dyksma et al., 2016). Moreover, the addition of MC somewhat limits the bioavailability of organic nitrogen in the system, resulting in a reduction of available resources within the environment and thereby triggering a deceleration in bacterial proliferation (Figure 5A).

Notably, the alteration of the environment may result in a relative increase in bacterial diversity (Figure 8). This is because deterministic processes tend to dominate in bacterial communities characterized by low diversity, whereas random occurrence may lead to the formation of more complex microbial co-occurrence networks (Zhu et al., 2024). In other words, when the addition of MC disrupts the original deterministic microbial community (Figure 9), the status of the dominant bacterium *Alphaproteobacteria* decreases, and in the absence of available resources in the environment, the microorganisms in the system compete with each other to proliferate, increasing bacterial diversity (Figure 5B). In the treatment group system, it is observed a gradual increase in the abundance of *Bacteroidia*, *Actinobacteria*, *Verrucomicrobiae* and *Planctomycetota* bacteria over time. This is due to their high competitiveness under resource-poor and aromatic-rich conditions (Liu et al., 2019; Li et al., 2020). These bacteria play important roles in degrading complex polysaccharides and proteins. For example, some *Actinobacteria* are capable of degrading polycyclic aromatic hydrocarbons (Dholakiya et al., 2017). *Verrucomicrobia* bacteria specialize in consuming

10.3389/fmars.2025.1558899

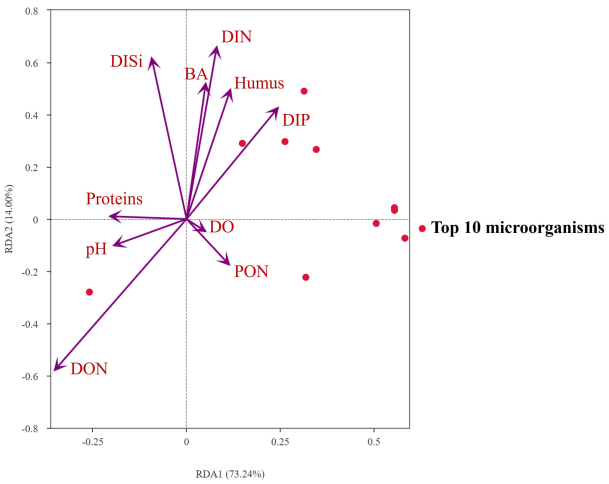

FIGURE 8
Correlation analysis of the microbial community with environmental factors.

difficult-to-degrade sulphate- and fructose-containing sugars. Compared with other bacteria, this group of bacteria prefers sugars that are difficult to degrade (Chiang et al., 2018; Orellana et al., 2022). Thus, we surmised that the bacterial breakdown of this organic matter with low bioavailability slowed the mineralization rate compared with that of highly bioavailable amino acids (Figure 2B), and the mineralization process of the whole system was prolonged, thus slowing the recycling and reuse of organic matter. Furthermore, in the prediction of bacterial function, the addition of MC decreased the correlation with the function of chemoheterotrophy bacterial (Figure 5E) and increased the correlation with the function of degrading low-bioavailable bacteria such as chitin and lignin. For example, the correlation with mineralization-related functional bacteria such as *Alphaproteobacteria* was reduced, and the correlation with functional bacteria related to the consumption of difficult-to-degrade nitrogenous organic matter such as *Verrucomicrobiae* was increased, which may slow the decomposition of nitrogenous organic matter, which in turn reduces the production of inorganic nutrient salts.

5 Conclusion

The MC can control HABs through flocculating and depositing HAB cells, while the subsequent mineralization was few studied. Here, we focused on the typical HAB organism *Skeletonema costatum* and investigated the effect of MC on the mineralization process. The results show that the addition of MC reduced both TON and DIN_{bulk} by 61% and 60%, respectively, and the mineralization rate decreased by 71% at the monthly scale. MC significantly reduced the mineralization rate of AON and mitigated the regeneration of inorganic nitrogen nutrients. At the same time, the increase in fluorescent dissolved organic matter and microbial abundance were both lower than the control group. The analysis suggested that MC may provide physical protection for organic nitrogen and form stable clay–organic matter complexes, increasing the difficulty of microbial decomposition and prolonging the mineralization time. In addition, MC alters the microbial community and triggers the growth of bacteria that preferentially degrade difficult-to-decompose organic nitrogen, which may be an important step in slowing the mineralization rates of AON and inhibiting the regeneration of inorganic nitrogen nutrients. This study provides a theoretical basis for evaluating the long-term

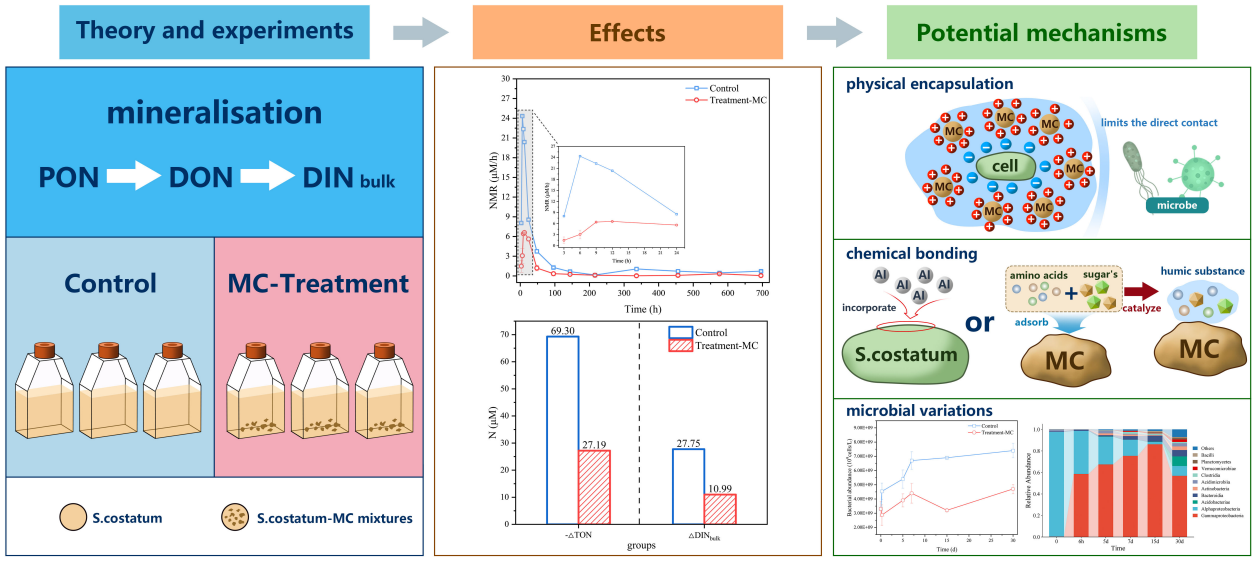

FIGURE 9
Mechanisms for mitigating AON mineralization processes in MC.

effects of MC treatments on HABs and provides a scientific reference for exploring the control mechanisms of marine organic matter mineralization, decomposition and burial.

Data availability statement

The original contributions presented in the study are included in the article/Supplementary Material. Further inquiries can be directed to the corresponding author.

Author contributions

XF: Data curation, Formal Analysis, Investigation, Methodology, Validation, Visualization, Writing – original draft, Writing – review & editing. WW: Conceptualization, Funding acquisition, Project administration, Supervision, Writing – review & editing. YC: Conceptualization, Writing – review & editing. JZ: Investigation, Methodology, Writing – review & editing. LC: Funding acquisition, Investigation, Methodology, Project administration, Writing – review & editing. JC: Validation, Visualization, Writing – review & editing. XS: Funding acquisition, Writing – review & editing. ZY: Project administration, Supervision, Writing – review & editing.

Funding

The author(s) declare that financial support was received for the research, and/or publication of this article. The financial support from the Intergovernmental innovation cooperation project of the Ministry of Science and Technology (2022YFE0136400), National Natural Science Foundation of China (42276220), and National Natural Science Foundation of China (42376210) to this work is gratefully acknowledged.

Acknowledgments

Authors would like to thank Qingdao University of Science and Technology and Institute of Oceanology, for their precious collaboration.

Conflict of interest

The authors declare that the research was conducted in the absence of any commercial or financial relationships that could be construed as a potential conflict of interest.

Generative AI statement

The author(s) declare that no Generative AI was used in the creation of this manuscript.

Publisher's note

Supplementary material

The Supplementary Material for this article can be found online at: https://www.frontiersin.org/articles/10.3389/fmars.2025.1558899/full#supplementary-material

References

Beck, L., Gehlen, M., Flank, A.-M., Van Bennekom, A. J., and Van Beusekom, J. E. E. (2002). The relationship between Al and Si in biogenic silica as determined by PIXE and XAS. *Nucl. Instruments. Methods Phys. Res. Section. B.: Beam. Interact. Mater. Atoms.* 189, 180–184. doi: 10.1016/S0168-583X(01)01035-7

Berman, T., and Bronk, D. (2003). Dissolved organic nitrogen: a dynamic participant in aquatic ecosystems. *Aquat. Microb. Ecol.* 31, 279–305. doi: 10.3354/ame031279

Bertilsson, S., and Jones, J. B. (2003). "1 - supply of dissolved organic matter to aquatic ecosystems: autochthonous sources," in *Aquatic Ecosystems*. Eds. S. E. G. Findlay and R. L. Sinsabaugh (Academic Press, Burlington), 3–24. doi: 10.1016/B978-012256371-3/50002-0

Bronk, D. A., See, J. H., Bradley, P., and Killberg, L. (2007). DON as a source of bioavailable nitrogen for phytoplankton. *Biogeosciences* 4, 283–296. doi: 10.5194/bg-4-283-2007

Cai, W.-J., Hu, X., Huang, W.-J., Murrell, M. C., Lehrter, J. C., Lohrenz, S. E., et al. (2011). Acidification of subsurface coastal waters enhanced by eutrophication. *Nat. Geosci.* 4, 766–770. doi: 10.1038/ngeo1297

Cappellen, P. V., Dixit, S., and van Beusekom, J. (2002). Biogenic silica dissolution in the oceans: Reconciling experimental and field-based dissolution rates. *Global Biogeochem. Cycles.* 16, 23–10. doi: 10.1029/2001GB001431

Catalá, T. S., Reche, I., Fuentes-Lema, A., Romera-Castillo, C., Nieto-Cid, M., Ortega-Retuerta, E., et al. (2015). Turnover time of fluorescent dissolved organic matter in the dark global ocean. *Nat. Commun.* 6, 5986. doi: 10.1038/ncomms6986

Chen, J., Li, H., Zhang, Z., He, C., Shi, Q., Jiao, N., et al. (2020). DOC dynamics and bacterial community succession during long-term degradation of Ulva prolifera and their implications for the legacy effect of green tides on refractory DOC pool in seawater. *Water Res.* 185, 116268. doi: 10.1016/j.watres.2020.116268

Chi, L., Ding, Y., He, L., Wu, Z., Yuan, Y., Cao, X., et al. (2022). Application of modified clay in intensive mariculture pond: Impacts on nutrients and phytoplankton. *Front. Mar. Sci.* 9. doi: 10.3389/fmars.2022.976353

Chi, L., Jiang, K., Ding, Y., Wang, W., Song, X., and Yu, Z. (2024). Uncovering nutrient regeneration, transformation pattern, and its contribution to harmful algal

blooms in mariculture waters. *Sci. Total. Environ.* 919, 170652. doi: 10.1016/j.scitotenv.2024.170652

Chiang, E., Schmidt, M. L., Berry, M. A., Biddanda, B. A., Burtner, A., Johengen, T. H., et al. (2018). Verrucomicrobia are prevalent in north-temperate freshwater lakes and display class-level preferences between lake habitats. *PloS One* 13, e0195112. doi: 10.1371/journal.pone.0195112

Coble, P. G. (1996). Characterization of marine and terrestrial DOM in seawater using excitation-emission matrix spectroscopy. *Mar. Chem.* 51, 325–346. doi: 10.1016/0304-4203(95)00062-3

Coble, P. G., Del Castillo, C. E., and Avril, B. (1998). Distribution and optical properties of CDOM in the Arabian Sea during the 1995 Southwest Monsoon. *Deep. Sea. Res. Part II.: Topical. Stud. Oceanogr.* 45, 2195–2223. doi: 10.1016/S0967-0645(98)00068-X

Dai, Y., Yang, S., Zhao, D., Hu, C., Xu, W., Anderson, D. M., et al. (2023). Coastal phytoplankton blooms expand and intensify in the 21st century. *Nature* 615, 280–284. doi: 10.1038/s41586-023-05760-y

Davidson, K., Gowen, R. J., Harrison, P. J., Fleming, L. E., Hoagland, P., and Moschonas, G. (2014). Anthropogenic nutrients and harmful algae in coastal waters. *J. Environ. Manage.* 146, 206–216. doi: 10.1016/j.jenvman.2014.07.002

Dholakiya, R. N., Kumar, R., Mishra, A., Mody, K. H., and Jha, B. (2017). Antibacterial and antioxidant activities of novel actinobacteria strain isolated from gulf of Khambhat, Gujarat. *Front. Microbiol.* 8. doi: 10.3389/fmicb.2017.02420

Ding, Y., Song, X., Cao, X., He, L., Liu, S., and Yu, Z. (2021). Healthier communities of phytoplankton and bacteria achieved via the application of modified clay in shrimp aquaculture ponds. *Int. J. Environ. Res. Public Health* 18, 11569. doi: 10.3390/ijerph182111569

Dixit, S., Van Cappellen, P., and Van Bennekom, A. J. (2001). Processes controlling solubility of biogenic silica and pore water build-up of silicic acid in marine sediments. *Mar. Chem.* 73, 333–352. doi: 10.1016/S0304-4203(00)00118-3

Dyksma, S., Bischof, K., Fuchs, B. M., Hoffmann, K., Meier, D., Meyerdierks, A., et al. (2016). Ubiquitous Gammaproteobacteria dominate dark carbon fixation in coastal sediments. *ISME. J.* 10, 1939–1953. doi: 10.1038/ismej.2015.257

Eusterhues, K., Rumpel, C., Kleber, M., and Kögel-Knabner, I. (2003). Stabilisation of soil organic matter by interactions with minerals as revealed by mineral dissolution and oxidative degradation. *Org. Geochem.* 34, 1591–1600. doi: 10.1016/j.orggeochem.2003.08.007

Exley, C., and Mold, M. J. (2015). The binding, transport and fate of aluminium in biological cells. *J. Trace Elements. Med. Biol.* 30, 90–95. doi: 10.1016/j.jtemb.2014.11.002

Feely, R. A., Alin, S. R., Newton, J., Sabine, C. L., Warner, M., Devol, A., et al. (2010). The combined effects of ocean acidification, mixing, and respiration on pH and carbonate saturation in an urbanized estuary. *Estuarine. Coast. Shelf. Sci.* 88, 442–449. doi: 10.1016/j.ecss.2010.05.004

Fuchs, G., Boll, M., and Heider, J. (2011). Microbial degradation of aromatic compounds — from one strategy to four. *Nat. Rev. Microbiol.* 9, 803–816. doi: 10.1038/nrmicro2652

Gibbs, R. J. (1983). Effect of natural organic coatings on the coagulation of particles. *Environ. Sci. Technol.* 17, 237–240. doi: 10.1021/es00110a011

Gonzalez, J. M., and Laird, D. A. (2004). Role of smectites and Al-substituted goethites in the catalytic condensation of arginine and glucose. *Clays. Clay. Miner.* 52, 443–450. doi: 10.1346/CCMN.2004.0520405

Goring, C., and Bartholomew, W. V. (1952). Adsorption of mononucleotides, nucleic acids, and nucleoproteins by clays. *Soil Sci.* 74, 149. doi: 10.1097/00010694-195208000-00005

Guo, J., Achterberg, E. P., Shen, Y., Yuan, H., Song, J., Liu, J., et al. (2023). Stable carbon isotopic composition of amino sugars in heterotrophic bacteria and phytoplankton: Implications for assessment of marine organic matter degradation. *Limnol. Oceanogr.* 68, 2814–2825. doi: 10.1002/lno.12468

He, S., Maiti, K., Ghaisas, N., Upreti, K., and Rivera-Monroy, V. H. (2023). Potential methane production in oligohaline wetlands undergoing erosion and accretion in the Mississippi River Delta Plain, Louisiana, USA. *Sci. Total. Environ.* 875, 162685. doi: 10.1016/j.scitotenv.2023.162685

Hemingway, J. D., Rothman, D. H., Grant, K. E., Rosengard, S. Z., Eglinton, T. I., Derry, L. A., et al. (2019). Mineral protection regulates long-term global preservation of natural organic carbon. *Nature* 570, 228–231. doi: 10.1038/s41586-019-1280-6

Huang, F., Lin, X., and Yin, K. (2022). Effects of algal-derived organic matter on sediment nitrogen mineralization and immobilization in a eutrophic estuary. *Ecol. Indic.* 138, 108813. doi: 10.1016/j.ecolind.2022.108813

Jenkinson, D. S. (1977). Studies on the decomposition of plant material in soil. V. The effects of plant cover and soil type on the loss of carbon from 14 C labelled ryegrass decomposing under field conditions. *J. Soil Sci.* 28, 424–434. doi: 10.1111/j.1365-2389.1977.tb02250.x

Jiao, N., Herndl, G. J., Hansell, D. A., Benner, R., Kattner, G., Wilhelm, S. W., et al. (2010). Microbial production of recalcitrant dissolved organic matter: long-term carbon storage in the global ocean. *Nat. Rev. Microbiol.* 8, 593–599. doi: 10.1038/nrmicro2386

Jiao, N., Herndl, G. J., Hansell, D. A., Benner, R., Kattner, G., Wilhelm, S. W., et al. (2011). The microbial carbon pump and the oceanic recalcitrant dissolved organic matter pool. *Nat. Rev. Microbiol.* 9, 555–555. doi: 10.1038/nrmicro2386-c5

Kirkham, D., and Bartholomew, W. V. (1954). Equations for following nutrient transformations in soil, utilizing tracer data. *Soil Sci. Soc. America J.* 18, 33–34. doi: 10.2136/sssaj1954.03615995001800010009x

Koning, E., Gehlen, M., Flank, A.-M., Calas, G., and Epping, E. (2007). Rapid post-mortem incorporation of aluminum in diatom frustules: Evidence from chemical and structural analyses. *Mar. Chem.* 106, 208–222. doi: 10.1016/j.marchem.2006.06.009

Kothawala, D. N., Kellerman, A. M., Catalán, N., and Tranvik, L. J. (2021). Organic matter degradation across ecosystem boundaries: the need for a unified conceptualization. *Trends Ecol. Evol.* 36, 113–122. doi: 10.1016/j.tree.2020.10.006

Landa, M., Cottrell, M. T., Kirchman, D. L., Kaiser, K., Medeiros, P. M., Tremblay, L., et al. (2014). Phylogenetic and structural response of heterotrophic bacteria to dissolved organic matter of different chemical composition in a continuous culture study. *Environ. Microbiol.* 16, 1668–1681. doi: 10.1111/1462-2920.12242

Laura, W. P., and Louca, S. (2016). Decoupling function and taxonomy in the global ocean microbiome. *Science* 353, 1272–1277. doi: 10.1126/science.aaf4507

Li, Y., Xu, C., Zhang, W., Lin, L., Wang, L., Niu, L., et al. (2020). Response of bacterial community in composition and function to the various DOM at river confluences in the urban area. *Water Res.* 169, 115293. doi: 10.1016/j.watres.2019.115293

Li, H., Zhang, Y., Liang, Y., Chen, J., Zhu, Y., Zhao, Y., et al. (2018). Impacts of maricultural activities on characteristics of dissolved organic carbon and nutrients in a typical raft-culture area of the Yellow Sea, North China. *Mar. pollut. Bull.* 137, 456–464. doi: 10.1016/j.marpolbul.2018.10.048

Liao, M. (2006). Effects of organic acids on adsorption of cadmium onto kaolinite, goethite, and bayerite. *Pedosphere* 16, 185–191. doi: 10.1016/S1002-0160(06)60042-8

Liu, S., Xi, B.-D., Qiu, Z.-P., He, X.-S., Zhang, H., Dang, Q.-L., et al. (2019). Succession and diversity of microbial communities in landfills with depths and ages and its association with dissolved organic matter and heavy metals. *Sci. Total. Environ.* 651, 909–916. doi: 10.1016/j.scitotenv.2018.09.267

Liu, H., Yuan, P., Liu, D., Zhang, W., Tian, Q., Bu, H., et al. (2021). Insight into cyanobacterial preservation in shallow marine environments from experimental simulation of cyanobacteria-clay co-aggregation. *Chem. Geol.* 577, 120285. doi: 10.1016/j.chemgeo.2021.120285

Lu, T., and Ji, M. (1996). Studies on dissolved amino acids in seawater of Jiaozhou Ba. *Oceanol. Limnol. Sin.* 27, 117–124.

Lu, G., Song, X., Yu, Z., and Cao, X. (2017). Application of PAC-modified kaolin to mitigate Prorocentrum donghaiense: effects on cell removal and phosphorus cycling in a laboratory setting. *J. Appl. Phycol.* 29, 917–928. doi: 10.1007/s10811-016-0992-3

Lu, G., Song, X., Yu, Z., Cao, X., and Yuan, Y. (2015). Effects of modified clay flocculation on major nutrients and diatom aggregation during *Skeletonema costatum* blooms in the laboratory. *Chin. J. Oceanol. Limnol.* 33, 1007–1019. doi: 10.1007/s00343-015-4162-2

Murphy, K. R., Stedmon, C. A., Graeber, D., and Bro, R. (2013). Fluorescence spectroscopy and multi-way techniques. PARAFAC. *Anal. Methods* 5, 6557–6566. doi: 10.1039/C3AY41160E

Noble, R. T., and Fuhrman, J. A. (1998). Use of SYBR Green I for rapid epifluorescence counts of marine viruses and bacteria. *Aquat. Microbial. Ecol.* 14, 113–118. doi: 10.3354/ame014113

Orellana, L. H., Francis, T. B., Ferraro, M., Hehemann, J.-H., Fuchs, B. M., and Amann, R. I. (2022). Verrucomicrobiota are specialist consumers of sulfated methyl pentoses during diatom blooms. *ISME. J.* 16, 630–641. doi: 10.1038/s41396-021-01105-7

Pekkonen, M., and Laakso, J. T. (2012). Temporal changes in species interactions in simple aquatic bacterial communities. *BMC Ecol.* 12, 18. doi: 10.1186/1472-6785-12-18

Pinck, L. A. (1962). "Adsorption of proteins, enzymes and antibiotics by montmorillonite," in *Clays and Clay Minerals*. Ed. E. Ingerson(Pergamon), 520–529. doi: 10.1016/B978-1-4831-9842-2.50041-9

Pinck, L. A., and Allison, F. E. (1951). Resistance of a protein-montmorillonite complex to decomposition by soil microorganisms. *Science*. 114 (2953), 130-131. doi: 10.1126/science.114.2953.130

Pivokonsky, M., Safarikova, J., Bubakova, P., and Pivokonska, L. (2012). Coagulation of peptides and proteins produced by Microcystis aeruginosa: Interaction mechanisms and the effect of Fe–peptide/protein complexes formation. *Water Res.* 46, 5583–5590. doi: 10.1016/j.watres.2012.07.040

Romera-Castillo, C., Sarmento, H., Álvarez-Salgado, X. A., Gasol, J. M., and Marrasé, C. (2011). Net production and consumption of fluorescent colored dissolved organic matter by natural bacterial assemblages growing on marine phytoplankton exudates. *Appl. Environ. Microbiol.* 77, 7490–7498. doi: 10.1128/AEM.00200-11

Salter, I., Böttjer, D., and Christaki, U. (2011). The effect of inorganic particle concentration on bacteria–virus–nanoflagellate dynamics. *Environ. Microbiol.* 13, 2768–2777. doi: 10.1111/j.1462-2920.2011.02547.x

Sigman, D. M., Casciotti, K. L., Andreani, M., Barford, C., Galanter, M., and Böhlke, J. K. (2001). A bacterial method for the nitrogen isotopic analysis of nitrate in seawater and freshwater. *Anal. Chem.* 73, 4145–4153. doi: 10.1021/ac010088e

Sorensen, L. H. (1981). Carbon-nitrogen relationships during the humification of cellulose in soils containing different amounts of clay. *Soil Biol. Biochem.* 13, 313–321. doi: 10.1016/0038-0717(81)90068-7

Stedmon, C. A., and Bro, R. (2008). Characterizing dissolved organic matter fluorescence with parallel factor analysis: a tutorial. *Limnol. Oceanogr. Methods* 6, 572–579. doi: 10.4319/lom.2008.6.572

Stedmon, C. A., Markager, S., and Bro, R. (2003). Tracing dissolved organic matter in aquatic environments using a new approach to fluorescence spectroscopy. *Mar. Chem.* 82, 239–254. doi: 10.1016/S0304-4203(03)00072-0

Testa, J. M., Brady, D. C., Di Toro, D. M., Boynton, W. R., Cornwell, J. C., and Kemp, W. M. (2013). Sediment flux modeling: Simulating nitrogen, phosphorus, and silica cycles. *Estuarine. Coast. Shelf. Sci.* 131, 245–263. doi: 10.1016/j.ecss.2013.06.014

Thornton, D. C. O. (2014). Dissolved organic matter (DOM) release by phytoplankton in the contemporary and future ocean. *Eur. J. Phycol.* 49, 20–46. doi: 10.1080/09670262.2013.875596

Wang, B., Chen, J., Jin, H., Li, H., Huang, D., and Cai, W.-J. (2017). Diatom bloom-derived bottom water hypoxia off the Changjiang estuary, with and without typhoon influence. *Limnol. Oceanogr.* 62, 1552–1569. doi: 10.1002/lno.10517

Yang, M., Liu, N., Wang, B., Li, Y., Li, W., Shi, X., et al. (2024). Stepwise degradation of organic matters driven by microbial interactions in China's coastal wetlands: Evidence from carbon isotope analysis. *Water Res.* 250, 121062. doi: 10.1016/j.watres.2023.121062

Yu, Z., Jingzhong, Z., and Xinian, M. (1994). Application of clays to removal of red tide organisms II. Coagulation of different species of red tide organisms with montmorillonite and effect of clay pretreatment. *Chin. J. Ocean. Limnol.* 12, 316–324. doi: 10.1007/BF02850491

Yu, Z., Song, X., Cao, X., and Liu, Y. (2017). Mitigation of harmful algal blooms using modified clays: Theory, mechanisms, and applications. *Harmful. Algae.* 69, 48–64. doi: 10.1016/j.hal.2017.09.004

Zhao, T., Xu, S., and Hao, F. (2023). Differential adsorption of clay minerals: Implications for organic matter enrichment. *Earth Sci. Rev.* 246, 104598. doi: 10.1016/j.earscirev.2023.104598

Zhou, Z., Lin, H., D'Sa, E. J., and Guo, L. (2024). A comparative study of optical and size properties of dissolved organic matter in the lower Mississippi River and Pearl River. *Mar. Chem.* 267, 104453. doi: 10.1016/j.marchem.2024.104453

Zhou, L., Liu, F., Liu, Q., Fortin, C., Tan, Y., Huang, L., et al. (2021a). Aluminum increases net carbon fixation by marine diatoms and decreases their decomposition: Evidence for the iron–aluminum hypothesis. *Limnol. Oceanogr.* 66, 2712–2727. doi: 10.1002/lno.11784

Zhou, L., Zhou, Y., Tang, X., Zhang, Y., Jang, K.-S., Székely, A. J., et al. (2021b). Resource aromaticity affects bacterial community successions in response to different sources of dissolved organic matter. *Water Res.* 190, 116776. doi: 10.1016/j.watres.2020.116776

Zhou, Y., Zhou, L., Zhang, Y., Garcia de Souza, J., Podgorski, D. C., Spencer, R. G. M., et al. (2019). Autochthonous dissolved organic matter potentially fuels methane ebullition from experimental lakes. *Water Res.* 166, 115048. doi: 10.1016/j.watres.2019.115048

Zhu, L., Luan, L., Chen, Y., Wang, X., Zhou, S., Zou, W., et al. (2024). Community assembly of organisms regulates soil microbial functional potential through dual mechanisms. *Glob. Change Biol.* 30, e17160. doi: 10.1111/gcb.17160